Metallophysics and Advanced Technologies
Металофіз. новітні технол.
Metallofiz. Noveishie Tekhnol.
2025, vol. 47, No. 4, pp. 405–414
https://doi.org/10.15407/mfint.47.04.0405
Reprints available directly from the publisher

PACS numbers: 61.72.sh, 61.82.Bg, 62.0.Qp, 62.80.+f, 68.35.Fx, 81.40.Ef, 81.70.Jb

Peculiarities of Atomic Migration in the Near-Surface Layers of the 2099 Al–Cu–Li Alloy during Ultrasonic Impact Treatment

O. V. Filatov[*], V. F. Mazanko[**], S. Ye. Bogdanov[*], B. M. Mordyuk[*], Ye. I. Bogdanov[*], S. P. Vorona[*], L. Kaczmarek[**], and M. Klich[***]

[*]*G. V. Kurdyumov Institute for Metal Physics, N.A.S. of Ukraine,*
36 Academician Vernadsky Blvd.,
UA-03142 Kyiv, Ukraine
[**]*Lodz University of Technology,*
116 Zeromskiego Str.,
90-924 Lodz, Poland
[***]*Institute of Security Technologies 'MORATEX',*
3 Marii Sklodowskiej-Curie Str.,
90-505 Lodz, Poland

The redistribution of ^{60}Co atoms in the near-surface layer 2099-T83 Al–Cu–Li alloy during ultrasonic impact treatment (UIT) is studied. As shown by microdurometric analysis, the UIT results in a significant hardening of 2099 Al–Cu–Li alloy. However, the increase in the UIT duration results in the microhardness decrease, which is explained by the stress-relaxation processes occurred in the alloy. The higher microhardness of the UIT-processed alloy is stable for more than a half year. The radioactive isotope technique reveals a nonmonotonic dependence of the ^{60}Co-atoms' distribution curves observed for the surface layers of the alloy samples UIT-processed for 60, 120 and 180 seconds. Moreover, the optimal mode is the UIT processing for 120 s. The calculated mass-transfer coefficients during UIT performed at room temperature match up the diffusion coefficients

Corresponding author: Oleksandr Valentynovych Filatov
E-mail: filatov@imp.kiev.ua

Citation: O. V. Filatov, V. F. Mazanko, S. Ye. Bogdanov, B. N. Mordyuk, Ye. I. Bogdanov, S. P. Vorona, L. Kaczmarek, and M. Klich, Peculiarities of Atomic Migration in the Near-Surface Layers of the 2099 Al–Cu–Li Alloy during Ultrasonic Impact Treatment, *Metallofiz. Noveishie Tekhnol.*, **47**, No. 4: 405–414 (2025). DOI: 10.15407/mfint.47.04.0405

known for the stationary homogenizing annealing at premelting temperatures. The mass-transfer coefficient value for ^{60}Co in 2099 Al–Cu–Li alloy during the room-temperature UIT exceeds the diffusion coefficient of ^{60}Co into aluminium at $T = 300$ K about $\cong 10^8$ times that indicates that the phenomenon of anomalous mass transfer is realized.

Key words: ultrasonic impact treatment, diffusion, mass transfer, radioactive isotope, deformation, microhardness.

Вивчено перерозподіл атомів ^{60}Co у приповерхневому шарі стопу 2099 Al–Cu–Li після термомеханічного оброблення Т83 за умов ультразвукового ударного оброблення (УЗУО). Методом мікродюрометричної аналізи показано, що УЗУО веде до істотного зміцнення стопу Al–Cu–Li 2099-Т83. Однак збільшення тривалости УЗУО призводить до зменшення мікротвердости, що пояснюється процесами релаксації напружень у стопі. Підвищена мікротвердість після УЗУО залишається стабільною у стопі понад півроку. Методом радіоактивних ізотопів було виявлено немонотонну залежність кривої розподілу ^{60}Co у стопі після ультразвукового ударного оброблення впродовж 60, 120 та 180 с, причому оптимальним режимом є час оброблення у 120 с. Коефіцієнти масоперенесення за умов УЗУО за кімнатної температури відповідають коефіцієнтам дифузії в умовах стаціонарного дифузійного відпалу за передтопильних температур. Величина коефіцієнта масоперенесення атомів ^{60}Co у стопі Al–Cu–Li 2099-Т83 під час УЗУО за кімнатної температури перевищує коефіцієнт дифузії ^{60}Co в алюміній за $T = 300$ К у $\cong 10^8$ разів, що свідчить про реалізацію явища аномального масоперенесення.

Ключові слова: ультразвукове ударне оброблення, дифузія, масоперенесення, радіоактивний ізотоп, деформація, мікротвердість.

(Received 18 December, 2024; in final version, 13 March, 2025)

1. INTRODUCTION

Spacecraft design methods and technologies are based on aircraft engineering principles. A greater emphasis is put on a weight minimization, vibration interactions, fatigue strength, and materials selection. The spacecraft design has to operate under conditions of static and dynamic loads occurred during testing and launch, and then in a zero-gravity environment [1].

The Al–Cu–Li alloys [2, 3] are widely used in aerospace engineering owing to the unique combination of low density, required strength and exceptionally high elastic moduli values compared to other aluminium alloys. Every percent of lithium reduces the density of the aluminium alloy by 3% and increases Young's modulus by 5%. The 2099 alloy of the Al–Cu–Li system has improved corrosion resistance and fatigue crack propagation properties in comparison with other alloys of this system. This alloy has the best set of mechanical, operational and anti-

corrosion properties, allowing it to compete in aerospace engineering with traditional aluminium alloys and polymer composite materials.

Optimum chemical composition of 2099 Al–Cu–Li alloys with a temper T83, where is solution heat-treated, strain hardened by 3%, then artificially aged [4] allow to obtain more favourable properties than previous generations of Al–Cu–Li alloys [5].

However, according to the literature data [6], the operational characteristics of 2099 Al–Cu–Li, namely, low density, increased elastic modulus, and high strength, were not significantly improved in comparison with other alloys of various series and modifications.

Therefore, the search and development of new techniques and processing methods allowing improving the physical-mechanical properties of Al–Cu–Li alloys for application in the aerospace industry is now an urgent task.

This work considers the mechanisms of atomic migration, microstructure evolution, and their influence on some mechanical properties of the near-surface layers in the 2099 Al–Cu–Li alloy of modification T83 under ultrasonic impact treatment (UIT).

2. EXPERIMENTAL DETAILS

The samples of 2099 Al–Cu–Li alloy made by Smiths (USA) and underwent a T83 temper involving solution heat treatment, water quenching and stretching prior to artificial ageing, in accordance with the accompanying factory technical certificates, has the following chemical composition: 2.6% Cu, 1.6% Li, 1% Zn (wt.%) and other elements of much less content (Mg 0.15, Mn 0.15, Ti 0.1, Zr < 0.1, Fe 0.07, Si 0.005) [7]. Additional chemical analysis [8] confirmed this percentage of chemical elements in the alloy. For the experiment, four samples were cut out (one initial and three for processing) with dimensions: 12×12×5 mm. A layer of the radioactive isotope ^{60}Co was electrolytically deposited onto the surface of three samples to be treated with ultrasonic impact treatment (UIT). The isotope layer thickness was $\cong 0.3$ μm and its activity was $\cong 5 \cdot 10^3$ imp/min. The radiation intensity is known to be directly proportional to the concentration of the ^{60}Co isotope.

The UIT process duration was chosen for each individual sample to be 60, 120, and 180 s. Ultrasonic impact treatment of 2099-T83 Al–Cu–Li alloy samples coated by ^{60}Co isotope was carried out at room temperature $\cong 300$ K in a step-like manner for 60 seconds each step to avoid UIT-induced overheating above 350 K [9]. Thus, the samples treated for 120 s and 180 s were cooled after every 60 s before continue the processing cycle. A detailed description and operating principles of the UIT equipment can be found in [10]. Parameters of the UIT: the oscillations' amplitude and frequency of the ultrasonic waveguide tip are 30 μm and 21 kHz, respectively, and the natural frequency of the im-

pact pin (*i.e.*, the frequency of the impact pulses) was of ≅ 0.5–1 kHz [11].

To obtain the depth profile of the concentration distribution of ^{60}Co isotope, the autoradiography and layer-by-layer removal techniques were used [12, 13]. The sample deformation extent was assessed as the ratio of the sample thicknesses measured before and after ultrasonic impact treatment [14]. The Vickers microhardness was measured using a microhardness tester. The plastic deformation rate ξ is determined by the formula [15]

$$\xi = \frac{\varepsilon}{\tau_{\text{eff}}}, \tag{1}$$

where ε is the relative plastic deformation of the sample, defined as the ratio of the sample thickness measured in the initial and treated states; τ_{eff} is the effective processing time.

3. RESULTS AND DISCUSSION

3.1. Microhardness

In this work, the microhardness (*HV*) values for the 2099-T83 Al–Cu–Li alloy samples in the initial state and after UIT process were measured at both the treated surface and backside. As shown, the microhardness of the initial sample is equal to 1.7 GPa; it increases to 5.47 GPa, 5.26 GPa, and 4.39 GPa after UIT lasted for 60 s, 120 s, and 180 s, respectively. Consequently, the UIT leads approximately to triple strain hardening of the alloy in comparison with the initial state. However, the microhardness is decreased with increasing of processing time, which indicates the occurrence of relaxation processes in the metal [16] (Table 1).

The deformation extent ε of the sample defined as the ratio of the sample thickness measured in the initial and processed states and after

TABLE 1. Values of relative deformation and microhardness of 2099-T83 Al–Cu–Li alloy before and after UIT.

$\tau_{\text{proc.}}$, s	ε, %	*HV*, GPa	$^{\text{bs}}HV$, GPa
initial	0	1.7	1.7
60	2.8	5.47	3.9
120	4.2	5.26	3.6
180	6.8	4.39	3.11
–	–	Al: 2.09 [17]	–

various UIT-processing times is given in Table 1 too. Analysis of these data shows that this dependence can be satisfactorily fitted by a linear function (Fig. 1). Thus, it is possible to interpolate the deformation extent for any other processing time. At the same time, it should be taken into account that the deformation extent is distributed non-homogeneously over the sample height and its maximum is near the sample surface. It leads to a slightly higher local heating, *i.e.*, to a higher probability of the recovery and dynamic recrystallization of the deformed microstructure in the near-surface region of the sample [18].

The backside microhardness of the sample (^{bs}HV) measured after UIT is changed similarly to the microhardness of the processed surface; however, its magnitude is lower. Approximately 2 times hardening is observed (*HV* increases up to 3.6–3.9 GPa; Table 1). The microhardness values induced by the room-temperature UIT process are revealed stable for more than six months.

3.2. Mass Transfer

In this work, the effect of the UIT duration on the migration and redistribution of atoms of the ^{60}Co isotope from the surface to the bulk of the 2099-T83 Al–Cu–Li alloy sample is considered. To calculate the plastic deformation rate and mass-transfer coefficient the UIT effective time (*i.e.*, the total time of the interaction between the impact striker and the surface of the Al–Cu–Li alloy) was taken into account. This UIT effective time is equal to a half of the total processing time [19]. Consequently, the time of effective processing ($\tau_{eff.proc.}$) was re-

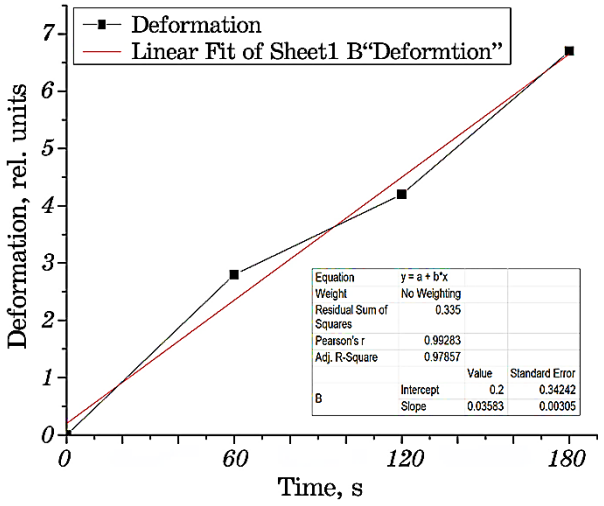

Fig. 1. Dependence of the deformation extent on the UIT duration.

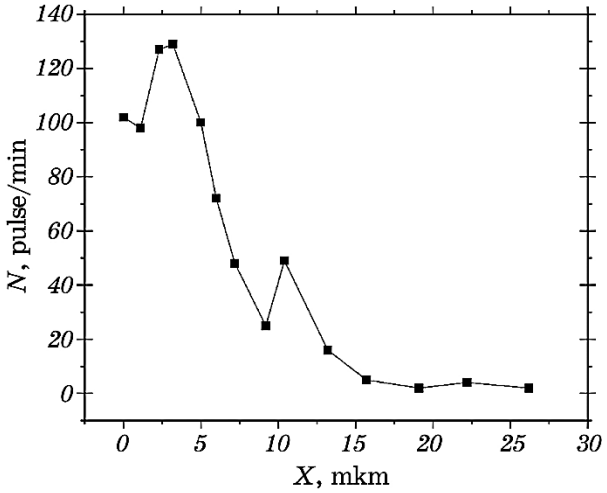

Fig. 2. Depth distribution of ^{60}Co isotope in 2099-T83 Al–Cu–Li alloy after UIT ($\tau_{proc.} = 60$ s).

spectively adopted to be 30 s, 60 s, and 90 s.

As can be seen in Fig. 2, the concentration distribution of the ^{60}Co isotope in 2099-T83 Al–Cu–Li alloy sample after UIT applied for 60 s has a non-monotonic character. Its feature is the presence of two maxima of the isotope concentration at a depth of about 3 μm and 11 μm.

The presence of the first maximum (3 μm) in the concentration profile is typical for the repeated pulse processing [20]. Moreover, it should be noted that the diffusion migration of atoms, as a rule, leads to appearing the stresses in crystals and to the formation of new dislocations [21]. As experimentally shown in Ref. [22], the physical nature of the first maximum of the isotope concentration (3 μm), related to plastic deformation, which leads to the accumulation of dislocations in this zone, and these dislocations can settle the diffusing atoms. The following continuation of processing generates more new dislocations, and the resulting stresses facilitate the diffusing atoms to overcome the dislocation barriers [19, 23]. The second maximum is located at a depth of about 11 μm. Apparently, the second maximum was formed for the same reason, due to the formation of a layer of the increased dislocation density. The mass-transfer coefficient estimated after UIT performed for effective processing time of 30 s achieved the value of $6.7 \cdot 10^{-8}$ cm^2/s.

Figures 3 and 4 show the experimental profiles of the ^{60}Co isotope distributions in 2099-T83 Al–Cu–Li alloy samples processed by after UIT for 120 s and 180 s, respectively. As seen, the regions with the increased concentration of isotope atoms at different depths are also observed.

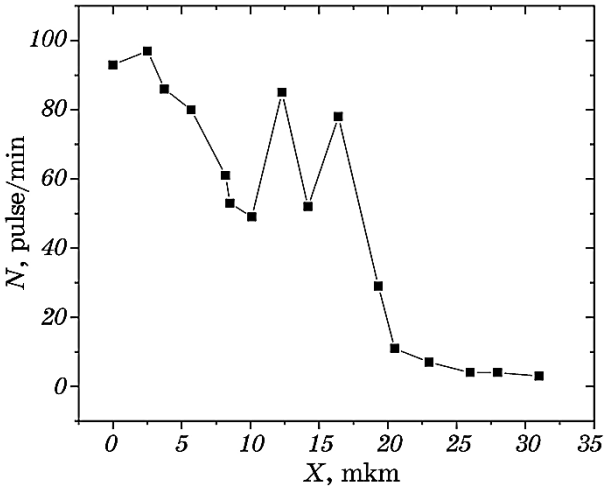

Fig. 3. Depth distribution of ^{60}Co isotope in 2099-T83 Al–Cu–Li alloy after UIT ($\tau_{proc.}$ = 120 s).

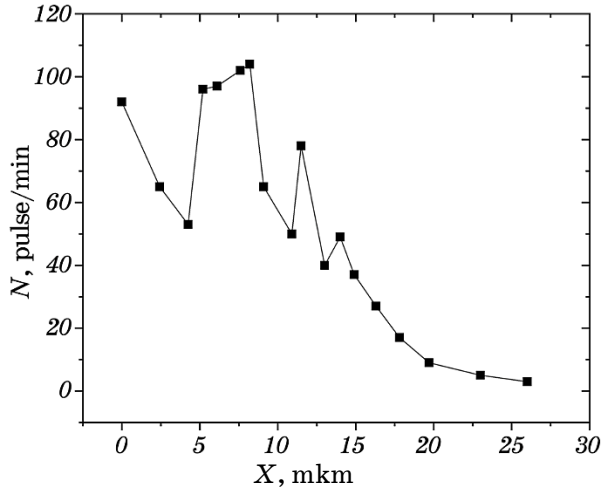

Fig. 4. Depth distribution of ^{60}Co isotope in 2099-T83 Al–Cu–Li alloy after UIT ($\tau_{proc.}$ = 180 s).

With the increase in the UIT duration, there is a continuous dynamic process of the structure rearrangement of the Al–Cu–Li alloy, with the unchanging strain rate (Table 2). During processing, even with a low strain rate (10^{-4}–10^{-6} s^{-1}), plastic deformation of alloy promotes the increase in the diffusion activity of impurity atoms on the surface and in the near-surface layers [21].

The most significant changes in the structural and concentration

TABLE 2. Data on the strain rate, mass-transfer coefficient *versus* the UIT duration of 2099-T83 Al–Cu–Li alloy.

No.	T, K	τ_{eff}, s	Depth, μm	ε, %	έ, s^{-1}	D_{eff}, cm^2/s
2099-T83 Al–Cu–Li	300	30	17	2.8	$9 \cdot 10^{-2}$	$6.7 \cdot 10^{-8}$
	300	60	26	4.2	$7 \cdot 10^{-2}$	$5.6 \cdot 10^{-8}$
	300	90	26	6.8	$7.6 \cdot 10^{-2}$	$3.5 \cdot 10^{-8}$
Co → Al (heterodiffusion)	910	–	–	–	–	$3.0 \cdot 10^{-8}$
$^{60}Co \rightarrow Al$	300	–	–	–	–	$5.0 \cdot 10^{-16}$

characteristics of the 2099-T83 Al–Cu–Li alloy during ultrasonic impact treatment applied for 60, 120, and 180 s are observed at the depth ranges in the near-surface layers of ≅ 5–15 μm deep. As seen in Figs. 2–4, the increase in the UIT duration from 60 s to 120 s leads to the increase in the penetration depth of the ^{60}Co isotope in the alloy sample. Further increase in the UIT duration to 180 s practically does not change the penetration depth. Therefore, in the UIT mode applied, it is advisable to use the processing time of 120 s.

The mass-transfer coefficients were calculated using Albert Einstein's formula [24]:

$$D_{eff} = \frac{x^2}{2\tau_{eff}} = \frac{(20)^2 \cdot 10^{-8}}{2 \cdot 30} = 6.7 \cdot 10^{-8} \frac{cm^2}{s}, \quad (2)$$

where x is the maximum penetration depth of diffusing atom, τ_{eff} is the effective duration of the UIT process.

The values of the mass-transfer coefficients calculated for the 2099-T83 Al–Cu–Li alloy samples at different UIT processing durations are presented in Table 2. For comparison, the heterodiffusion coefficient of Co into aluminium during stationary annealing are also presented there [13].

As can be seen from Table 2, the mass-transfer coefficient gradually decreases with the increasing UIT process duration. At the UIT lasted for 60 s, 120 s, and 180 s, the $^{60}Co \rightarrow$ Al–Cu–Li mass-transfer coefficients are comparable to the Co → Al heterodiffusion coefficient known for stationary annealing at 910 K. At the same time, the value of the diffusion coefficient of $^{60}Co \rightarrow Al$ at room temperature (obtained by extrapolation) gives a value of $5.0 \cdot 10^{-16}$ cm^2/s. The D_M/D ratio is of $7 \cdot 10^9$ times, *i.e.*, in this case, the phenomenon of anomalous mass transfer is realized not due to the temperature exposure, but owing to the presence of a driving force induced by the impact (pulse) mechanical action on the 2099-T83 Al–Cu–Li alloy driven by UIT. It can be assumed that the nature of the driving force involves an increase of pen-

etrating-atoms' quantity promoted by moving dislocations. This phenomenon was observed in works [19, 23].

CONCLUSIONS

1. The linear increase in the plastic deformation extent with increasing time of the ultrasonic impact treatment from 60 to 180 seconds is observed.
2. The UIT process leads to three times microhardness increase of 2099-T83 Al–Cu–Li alloy. The higher microhardness value obtained after the UIT is stable for more than a half of year.
3. The nonmonotonic dependence of the ^{60}Co concentration distribution in 2099-T83 Al–Cu–Li alloy after ultrasonic impact treatment is observed.
4. The increase in the UIT duration from 60 s to 120 s results in the increase in of penetration depth of ^{60}Co isotope in 2099-T83 Al–Cu–Li alloy. Further increase in the UIT process duration to 180 s does not change the penetration depth. Therefore, in the applied UIT mode, it is advisable to use a processing time of 120 s.
5. The mass-transfer coefficients at the room temperature UIT match up the diffusion coefficients known for the stationary homogenizing annealing at premelting temperatures.
6. The most significant changes in the structural and concentration characteristics of 2099-T83 Al–Cu–Li alloy at UIT lasted for 60, 120, and 180 s are observed in the near-surface layers at the depths of $\cong$ 5–15 μm.
7. The mass-transfer coefficient magnitude for the 2099-T83 Al–Cu–Li alloy at the room temperature UIT exceeds the diffusion coefficient $^{60}\text{Co} \rightarrow \text{Al}$ at $T = 300$ K by $\cong 10^8$ times that indicates the realization of the phenomenon of anomalous mass transfer.

The work is carried out within the framework of R&D (Reg. No. 0122U002366) supported by the National Academy of Sciences of Ukraine, which is gratefully acknowledged.

REFERENCES

1. E. A. Starke and J. T. Staley, *Prog. Aerosp. Sci.*, **32**: 131 (1996).
2. A. M. Abd El-Hameed and Y. A. Abdel-Aziz, *J. Adv. Res. Appl. Sci. Eng. Technol.*, **22**, No. 1: 1 (2021).
3. I. J. Polmear, *Mater. Trans. JIM*, **37**, No. 1: 12 (1996).
4. Y. Lin, Z. Zheng, S. Li, X. Kong, and Y. Han, *Mater. Charact.*, **84**: 88 (2013).
5. R. J. Rioja and J. Liu, *Metall. Mater. Trans. A*, **43**, No. 9: 3325 (2012).
6. E. Balducci, L. Ceschini, S. Messieri, S. Wenner, and R. Holmestad, *Mater. Design*, **119**: 54 (2017).
7. https://www.smithshp.com/pdf/2099-aluminium-lithium.pdf

8. Ya. G. Goroshchenko, *Fiziko-Khimicheskiy Analiz Gomogennykh i Geterogennykh Sistem* [Physicochemical Analysis of Homogeneous and Heterogeneous Systems] (Kiev: Naukova Dumka: 1978) (in Russian).
9. P. Yu. Volosevich, G. I. Prokopenko, and B. M. Mordyuk, *Metallofiz. Noveishie Tekhnol.*, **22**, No. 9: 61 (2000) (in Russian).
10. B. N. Mordyuk and G. I. Prokopenko, Ultrasonic Impact Treatment—An Effective Method for Nanostructuring the Surface Layers in Metallic Materials, *Handbook of Mechanical Nanostructuring* (Ed. M. Aliofkhazraei) (Wiley-VCH: Verlag, 2015).
11. S. P. Chenakin, B. M. Mordyuk, N. I. Khripta, and V. Yu. Malinin, *Metallofiz. Noveishie Tehnol.*, **45**, No. 9: 1109 (2023).
12. J. F. Babikova, A. A. Gusakov, V. M. Minajev, and G. G. Rjabova, *Analitycheskaya Avtoradiographiya* [Analytical Autoradiography] (Moskva: Energoatomizdat: 1985) (in Russian).
13. L. N. Larikov and V. I. Isaichev, *Diffuziya v Metallakh i Splavakh: Spravochnik* [Diffusion in Metals and Alloys: Handbook] (Kiev: Naukova Dumka: 1987) (in Russian).
14. P. L. Moore and G. Booth, *The Welding Engineer's Guide to Fracture and Fatigue. 1st Edition* (Woodhead Publishing Series in Metals and Surface Engineering) (November 3, 2014).
15. J. Hirth and J. Lothe, *Theory of Dislocations* (Krieger Publishing Company: 1982).
16. G. I. Eskin and D. G. Eskin, *Ultrasonic Treatment of Light Alloy Melts. 2nd Edition* (Boca Raton: CRC Press: 2017).
17. S. Renwick, *Handbook of Aluminium Alloys. Illustrated Edition* (New York: Research Press: March 5, 2015).
18. Y. Tang, D. H. Xiao, L. P. Huang, R. X. You, X. Y. Zhao, N. Lin, Y. Z. Ma, and W. S. Liu, *Mater. Charact.*, **191**: 112135 (2022).
19. O. M. Soldatenko, O. V. Filatov, B. M. Mordyuk, and S. M. Soldatenko, *Metallofiz. Noveishie Tekhnol.*, **45**, No. 1: 65 (2023).
20. D. S. Gertzriken, V. F. Mazanko, V. M. Tyshkevich, and V. M. Falchenko, *Massoperenos pri Nizkikh Temperaturakh v Usloviyakh Vneshnikh Vozdeistviy* [Mass Transfer at Low Temperatures under External Influences] (Kiev: RIO IMF: 2001) (in Russian).
21. S. D. Gertzriken and I. Ya. Dekhtyar, *Diffuziya v Metallakh i Splavakh v Tverdoy Faze* [Diffusion in Metals and Alloys in the Solid Phase] (Moskva: GIFML: 1960) (in Russian).
22. V. M. Mironov, V. F. Mazanko, D. S. Gertzriken, and O. V. Filatov, *Massoperenos i Fazoobrazovanie v Metalakh pri Impulsnykh Vozdeistviyakh* [Mass Transfer and Phase Formation in Metals under Pulsed Influences] (Samara: Samarskiy Universitet: 2001) (in Russian).
23. A. Filatov, A. Pogorelov, D. Kropachev, and O. Dmitrichenko, *Defect. Diffus. Forum*, **363**: 173 (2015).
24. J. R. Manning, *Diffusion Kinetics for Atoms in Crystals* (Princeton, NJ: D. Van Nostrand Co., Inc.: 1968).